Multiobjective Optimization of an Industrial Semibatch Nylon 6 Reactor

RAJIV SAREEN and SANTOSH K. GUPTA*

Department of Chemical Engineering, Indian Institute of Technology, Kanpur - 208016, India

SYNOPSIS

Multiobjective Pareto optimal solutions have been generated for three grades of nylon 6 being produced in an industrial semibatch reactor. The optimal operating conditions (called preferred solutions) for these three batches are easy to implement and lead to substantial improvements over current practice. The technique used is quite general and can easily be applied to improve the operation of other industrial polymerization reactors or design better (new) reactors. Good mathematical models, which account for the important physicochemical aspects actually operative in a reactor and which have been tested on industrial data, are a prerequisite for such optimization studies. © 1995 John Wiley & Sons, Inc.

INTRODUCTION

As in other systems, the operating variables in a polymerization reactor influence its performance in interesting but often conflicting ways. This necessitates their optimization and a study of their parametric sensitivity. A number of studies have been reported in the past on the optimal temperature and initiator or monomer addition histories (or profiles) for free-radical[1-5] and step-growth polymerizations[5-14] in batch, semibatch, or plug-flow reactors. In most of these studies, the function which is minimized (or maximized) is the weighted average of a few individual objectives, selected, e.g., from among the (a) concentration of unreacted monomer in the product, (b) concentration of undesirable side products, (c) reaction time, (d) deviation of the number-average chain length (μ_n), and/or polydispersity index (PDI), from the desired values, etc. The, scalar (overall) objective functions, I, used in these studies are, thus, of the form

$$\underset{\mathbf{u}(t)}{\text{Min}}\ I = \sum_i w_i I_i[\mathbf{x}(t_f), t_f] \qquad (1)$$

In eq. (1), w_i is the weightage factor associated with the individual objective function, I_i; $\mathbf{u}(t)$, the control variable history (in general, a vector representing, e.g., temperature, initiator addition rate); t, the time; t_f, the (final) reaction time; and $\mathbf{x}(t)$, the vector of state variables describing the system. The optimal histories (or profiles) were generated using a variety of constraints, e.g., the reaction temperature being limited between an upper and a lower bound, etc.

Computation of the optimal trajectories, $\mathbf{u}(t)$, of the type described is relatively simple, but there is considerable subjectivity on the values assigned to the weightage factors. Mathematically, the most important drawback of this approach is the possibility of losing certain optimal solutions,[15,16] irrespective of the weightage factors used in the (overall) objective function, I. This happens[15,16] when the nonconvexity of the objective function gives rise to a duality gap. Since real-life problems are seldom convex, an alternative approach, if possible, needs to be explored.

In recent years, the area of *vector* optimization has come into prominence in polymer engineering. In this, the objective function, $\mathbf{I}$, is a vector comprising the individual objective functions, I_i. This is a very powerful approach and leads to better decision making by a designer. This method has its roots[15,16] in management science and resource management and is referred to as multiobjective decision making or optimization. It not only overcomes the disadvantages associated with scalar optimization,

* To whom correspondence should be addressed.

Journal of Applied Polymer Science, Vol. 58, 2357–2371 (1995)
 CCC 0021-8995/95/132357-15

but offers additional advantages of being able to deal with usually incompatible and nonquantifiable effects like pollution, efficiency, etc. Since most optimization problems in polymer reaction engineering often deal with such objectives, multiobjective function optimization offers excellent prospects for use in the optimal design and operation of these reactors. Indeed, a few studies[17-21] have already been reported in the last decade on the optimization of polymer and copolymer reactors using this methodology. None of these studies, however, was on industrial reactors, even though the qualitative conclusions drawn can give valuable insight. In this article, we optimize the operation of an *industrial* semibatch nylon 6 reactor. This reactor has been simulated by our group earlier,[22-24] and a satisfactory mathematical model is already available, which can be used with confidence for optimization purposes.

Multiobjective function optimization is usually executed in two phases—an objective or mathematical phase and a subjective or decision-making phase. In the mathematical phase, a Pareto set is generated. This is a set of equivalent optimum points, such that upgrading any one objective function leads to simultaneous worsening of at least one or more other objective functions. The points on the Pareto set satisfy all the constraints of the problem, e.g., mass and energy balance equations (usually in the form of ordinary differential equations [ODEs] for well-mixed reactors) and end-point constraints (e.g., product having a desired value of μ_n). Each point on the Pareto corresponds to a different operating (or control) variable history, $\mathbf{u}(t)$. The second phase is slightly more subjective in nature and involves the decision maker to study the "best" of the optimal points on the Pareto set, using his "judgement" (or additional information not incorporated in the generation of the Pareto and usually not easily quantifiable). It is obvious that the Pareto set generated in phase 1 helps channelize the thinking of the decision maker in a better manner.

Several methods have been described in the literature on the generation of the Pareto set. Of these, the simplest and the most commonly used is the ε-constraint approach. In this,[15,16] we select any one objective function and minimize it while constraining the remaining objectives to have some preassigned values, ε_j. Thus, the original multivariable optimization described by

$$\underset{\mathbf{u}(t)}{\text{Min}}\ \mathbf{I}[\mathbf{x}(t_f), t_f] = \underset{\mathbf{u}(t)}{\text{Min}}\ [I_1[\mathbf{x}(t_f), t_f], I_2[\mathbf{x}(t_f), t_f], \ldots, I_r[\mathbf{x}(t_f), t_f]] \quad (2a)$$

subject to (s. t.):

all constraints [e.g., mass and energy balances, end-point constraints, maximum and minimum values on $\mathbf{u}(t)$, etc.] (2b)

is transformed into the following simpler problem:

$$\underset{\mathbf{u}(t)}{\text{Min}}\ I_i[\mathbf{x}(t_f), t_f] \quad (3a)$$

s.t.:

$$I_j[\mathbf{x}(t_f), t_f] = \varepsilon_j;\ j = 1, 2, \ldots, r; \quad j \neq i \quad (3b)$$

all other constraints [as in eq. 2(b)] (3c)

The solution of the problem described in eq. (3) gives a single point on the Pareto set. The complete Pareto surface can be generated by varying ε_j over their entire range, $\varepsilon_{j,\min}$ to $\varepsilon_{j,\max}$. The values of $\varepsilon_{j,\min}$ or $\varepsilon_{j,\max}$ can be obtained by the solution of the following still *simpler* problems:

$$\varepsilon_{j,\max} = \underset{\mathbf{u}(t)}{\text{Max}}\ I_j[\mathbf{x}(t_f), t_f] \quad (4a)$$

s.t.:

all constraints in the original problem [eq. 2(b)] (4b)

and

$$\varepsilon_{j,\min} = \underset{\mathbf{u}(t)}{\text{Min}}\ I_j[\mathbf{x}(t_f), t_f] \quad (5a)$$

s.t.:

all constraints in the original problem [eq. 2(b)] (5b)

Each point of the Pareto set has an optimal history, $\mathbf{u}(t)$, associated with it. These are generated simultaneously while obtaining the solutions of the problems described in eq. (3), using various techniques, e.g., dynamic programming, iterative dynamic programming, and Pontryagin's principle using first- or second-order techniques.

The generation of the Pareto set completes the first or objective phase of the problem. This is followed by the subjective or the decision-making phase involving the decision makers. The techniques[15,16]

used to decide upon the best of the equivalent optimal points on the Pareto set are described later in this article for the example studied herein.

The industrial reactor[22-24] which has been optimized in the present study is shown schematically in Figure 1. The reactor is a jacketed vessel equipped with a low-speed anchor or ribbon agitator for mixing the reaction mass. A liquid mixture of caprolactam and water (along with other inert additives like TiO_2, etc.) is heated by condensing vapors in the jacket. Polymerization takes place in the liquid phase, as the temperature goes above 220°C, and some water and caprolactam vaporize. The pressure above the liquid reaction mixture is manipulated by a control valve which releases the vapor mixture of nitrogen (inert), monomer, and water to a condenser at a prescribed rate so as to maintain a desired pressure history, $p(t)$, in the reactor. The pressure history used presently (termed as reference [ref]) is shown schematically in Figure 2 (curve ref), using the following dimensionless variables:

$$\Pi \equiv (p - p_0)/(p_{\max,\text{ref}} - p_0)$$
$$\tau \equiv t/t_{f,\text{ref}} \tag{6}$$

Values of $p_{\max,\text{ref}}$ and $t_{f,\text{ref}}$ are not being given for proprietary reasons.

The operation of the reactor at present (ref) can be described in terms of five stages (Fig. 2). In the first stage, the reaction mass is heated gradually to about 250–270°C. During this time, the control valve is kept closed and the pressure is allowed to build up to a desired, maximum value, $p_{\max,\text{ref}}$. In stage 2, the valve opens and releases vapor at such a rate so that the pressure remains constant at $p_{\max,\text{ref}}$ for a

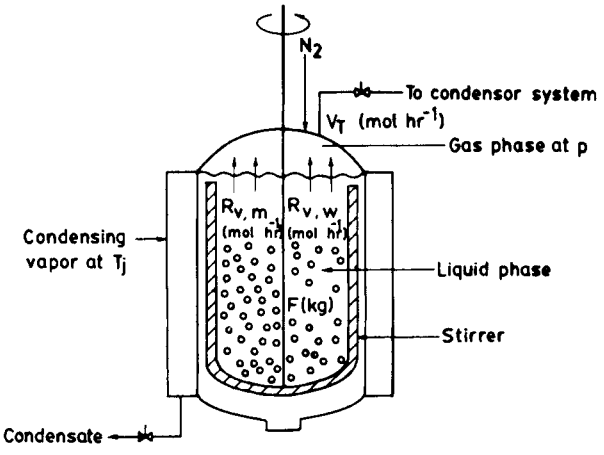

Figure 1 Schematic representation of the industrial semibatch nylon 6 reactor.

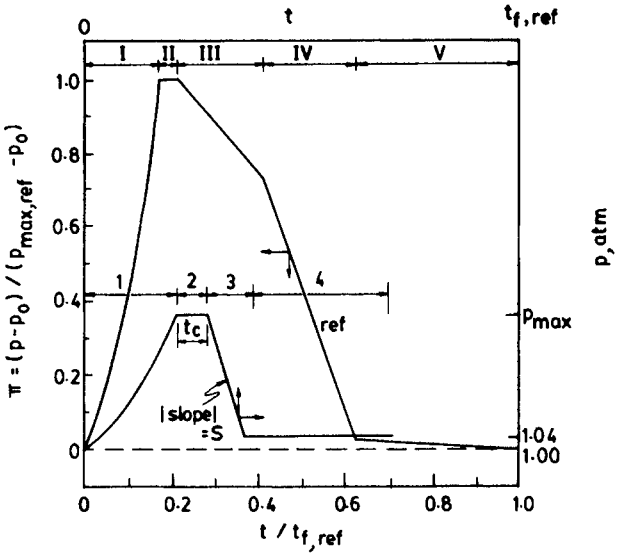

Figure 2 Schematic pressure histories for the semibatch reactor. Curve (ref): current industrial practice; (O) history for optimization purposes.

short period of time, $t_{c,\text{ref}}$. In the third, fourth, and fifth stages, the control valve is operated such that the pressure drops linearly (at different rates), finally reaching a value slightly above atmospheric (to prevent leakage into the reactor) at the end of the fifth stage. By this time, the polymerization is complete, and the contents of the reactor are emptied for further processing (cooling to below the melting point of nylon 6, hot-water extraction, pelletizing, etc.).

In this industrial reactor, the jacket fluid temperature is maintained constant with time. Details of the model used, some operating conditions, the simulated temperature and pressure histories for $0 \le t \le t_{f,\text{ref}}$, and the simulated pressure history in the first zone (which is determined by the rate of vaporization of monomer and water) are available in Ref. 24, and the computed results are found to compare well with industrial data for three different polymerization runs.[24] This model is used without any change for multifunction optimization.

FORMULATION

Two objective functions were selected in this study for minimization:

(i) The dimensionless reaction time, $t_f/t_{f,\text{ref}}$: The residence time is determined by the time required for the degree of polymerization, μ_n, to reach a value, $\mu_{n,\text{ref}}$, being obtained presently in the industrial reactor. This ensures

the quality of the product in terms of its physical properties. This requirement is termed as a stopping condition, since the integration of the model equations (ODEs) terminates when $\mu_{n,f} \equiv \mu_n(t_f) = \mu_{n,\text{ref}}$.

(ii) The nondimensional concentration of the undesirable cyclic compounds in the polymer produced: Since cyclic dimer formation predominates over the production of higher cyclic oligomers, we minimize $[C_2]_f/[C_2]_{f,\text{ref}}$. The cyclics cause problems in polymer processing and hot-water extraction is used to remove them.[25] Since this operation is expensive and energy-intensive, minimization of the final cyclic dimer concentration is important. It is to be noted that $t_{f,\text{ref}}$ and $[C_2]_{f,\text{ref}}$ are constants and their inclusion in the individual objective functions does not influence the results of the study in any way.

The above objective functions are incompatible,[12] since trying to minimize one of them may lead to larger values of the other. Hence, there is a definite advantage in resorting to multiobjective function optimization. The jacket fluid temperature, T_j (constant), and the vapor-release rate history, $V_T(t)$, are the operating variables for this industrial reactor, and so should be taken as the control variables. Another constraint that we would like to meet is that the final monomer conversion, conv_f, remains at the value, $\text{conv}_{f,\text{ref}}$, obtained presently. This will ensure no additional load on the follow-up units in the industry, where the unreacted monomer has to be leached out and suitably disposed of (or recycled). The monomer conversion in a semibatch reactor at any time, t, is defined as

$$\text{conv} = 1.0 - (F[C_1] + \zeta_1)/(F_0[C_1]_0) \qquad (7)$$

where F and $[C_1]$ represent the mass of the liquid reaction mixture and the concentration (mol/kg) of the monomer at any time, respectively, and 0 represents the initial values. ζ_1 is the (cumulative) amount (mol) of monomer that has vaporized until time t. Correcting for monomer vaporization in this way is quite common and useful for semibatch reactor operation. Thus, the optimization problem being solved in the present study is defined by

$$\underset{T_j, V_T(t)}{\text{Min}} \; \mathbf{I} \equiv \left[\frac{t_f}{t_{f,\text{ref}}}, \frac{[C_2]_f}{[C_2]_{f,\text{ref}}} \right] \qquad (8a)$$

s.t.:

$$\mu_{n,f} = \mu_{n,\text{ref}} \qquad (8b)$$

$$\text{conv}_f = \text{conv}_{f,\text{ref}} \qquad (8c)$$

$$\text{mass and energy balance equations} \qquad (8d)$$

any additional limits

$$\text{put on control variables} \qquad (8e)$$

We now discuss eqs. 8(d) and 8(e) in more detail. The reactor is described by a set of ordinary differential equations representing the mass and energy balances, as well as by the equations for the moments of the chain-length distribution of the polymer formed. These are given in Ref. 24, in the form $dx_i/dt = f_i(\mathbf{x})$, along with several auxillary algebraic equations to estimate the rates of heat and mass transfer (vaporization). These are to be used in eq. 8(d). The backward difference formulas for stiff equations[26] are used to integrate these ODEs. This was done using the D02EJF subroutine of the NAG library, using a relative error tolerance, TOL, of 10^{-6}. The model predicts how several important quantities evolve with time, as well as their final values. These include the number-average molecular weight or degree of polymerization (μ_n), PDI, water extractibles, cyclic dimer concentration, monomer conversion, etc. Also, characteristics like heat and mass transfer rates, viscosity of the reaction mass, pressure in zone 1 (when the control valve is closed, i.e., $V_T = 0$), etc., are predicted for a specified feed and given values of T_j, as well as the pressure histories, $p(t)$, in zones 2–5.

Solving the multiobjective optimization problem described in eq. (8) requires the use of Pontryagin's minimum principle[27] to obtain optimal histories of $V_T(t)$. This is not too easy a task for the industrial problem being studied here, and, indeed, our early attempts failed due to computational problems. A few exploratory *simulation* runs with different $V_T(t)$ and $p(t)$ histories were made to see if the problem could be reformulated (while still being useful to industry). It was inferred that we could choose T_j and $p(t)$ as the control variables instead of T_j and $V_T(t)$. In fact, we could freeze the *shape* of $p(t)$, use a few parameters (constants) to describe this history, and then obtain optimal values for these parameters. The mathematical and numerical problems associated with this modified problem are far less. The *shape* of the pressure history used for optimization is described completely in terms of only four stages (instead of five as being used currently):

(a) The pressure builds up from 1 atm to $p_{\max}$ during $0 \le t \le t_1$, the valve being closed ($V_T = 0$) during the first stage.

(b) The pressure is maintained constant at p_{max} during $t_1 \le t \le t_1 + t_c$.

(c) The pressure decreases with slope S (i.e., $dp/dt = -S$), until p becomes 1.04 atm. Thus, stage 3 extends over $t_1 + t_c \le t \le t_1 + t_c + (p_{max} - 1.04 \text{ atm})/S$.

(d) The pressure is maintained at 1.04 atm until μ_n reaches the desired value, $\mu_{n,ref}$. At this point, $t = t_f$.

We see that the optimal pressure history can be described by only three (constant) parameters, p_{max}, S, and t_c (t_1 and t_f being computed from the model equations). Figure 2 shows this pressure history schematically. The $V_T(t)$ history in stages 2, 3, and 4 can be *evaluated* from the model once the optimal $p(t)$ is known. The control variables for this new optimization problem are, thus, p_{max}, S, t_c, and T_j, all being constants whose *values* are to be determined.

The modified optimization problem is described by

$$\text{Min } \mathbf{I}(p_{max}, S, t_c, T_j) = \left[\frac{t_f}{t_{f,ref}}, \frac{[C_2]_f}{[C_2]_{f,ref}}\right] \quad (9a)$$

s.t.:

$$\mu_1(t_f) = \mu_{n,ref}\,\mu_0(t_f) \quad \text{(stopping condition)} \quad (9b)$$

$$\text{conv}_f = \text{conv}_{f,ref} \quad (9c)$$

$$\frac{d\mathbf{x}}{dt} = \mathbf{f}[\mathbf{x}(t), p_{max}, S, t_c, T_j];$$

$$\mathbf{x}(t = 0) = \mathbf{x}_0 \quad \text{(from Ref. 24)} \quad (9d)$$

$$p_{max}/p_{max,ref} \le 1.0 \quad (9e)$$

$$0 \le S/S_{max,ref} \le 1.0 \quad (9f)$$

$$0.0 \le t_c/t_{f,ref} \le 0.1875 \quad (9g)$$

$$0.8703 \le T_j/563 \text{ K} \le 1.0 \quad (9h)$$

where $\mu_0(t)$ and $\mu_1(t)$ are the zeroth and first moments of the chain-length distribution at any time, t.

It may be noted that several minimum/maximum value constraints on the control parameters, p_{max}, S, t_c, and T_j, have been included in eq. (9), again in a dimensionless form. Equation 9(e) is a reasonable constraint to use for the existing reactor since we did not wish to exceed the pressure rating of the industrial reactor. Equation 9(f) on S, indirectly, puts some kind of an upper limit on the rate of release of vapors, V_T. It is unlikely that the existing control valve can accommodate *much* higher vapor release rates than the current value. The upper limit on t_c [eq. (9g)] has been taken to be about twice the maximum value being used currently. The lower limit on T_j [Eq. (9h)] is the melting point of nylon 6, while the upper limit is about 20°C higher than the current jacket fluid temperature. The upper limits imposed on t_c and T_j are purely for ease of computation, since the optimal values of these parameters lie away from these bounds.

For generating the Pareto, the ε-constraint approach applied to eq. (9) necessitates the solution of the following problem:

$$\text{Min } I_2(p_{max}, S, t_c, T_j) = [C_2]_f/[C_2]_{f,ref} \quad (10a)$$

s.t.:

$$\frac{t_f}{t_{f,ref}} = \varepsilon \quad (10b)$$

$$\text{constraint eqs. (9b)–(9h)} \quad (10c)$$

The range of $t_f/t_{f,ref}$ to be explored (i.e., the range of ε) is determined by solving the two simpler optimization problems described by

$$\text{Min } I_1(p_{max}, S, t_c, T_j) = t_f/t_{f,ref} \quad (11a)$$

s.t.:

$$\text{constraint eqs. (9b)–(9h)} \quad (11b)$$

and

$$\text{Min } I_2(p_{max}, S, t_c, T_j) = [C_2]_f/[C_2]_{f,ref} \quad (12a)$$

s.t.:

$$\text{constraint eqs. (9b)–(9h)} \quad (12b)$$

The above three optimization problems [eqs. (10)–(12)] are solved using the E04UCF code of the NAG library. This code is designed to solve the nonlinear programming (NLP) problem. It minimizes a single, smooth function, $\mathcal{F}(\mathbf{x})$, of n state variables, $\mathbf{x}$, subject to constraints which may include n simple bounds on the state variables, n_L, linear, and n_{nl}, smooth, nonlinear constraints involving $\mathbf{x}$. It uses a sequential quadratic programming (SQP) algorithm, as developed by Gill et al.[28,29] The method first determines a feasible point which satisfies all the constraints. Then, in each iteration, it

Table I Initial Guesses for Generation of First Point on the Pareto Sets

Problem No.	$[W]_0$	$\mu_{n,\text{ref}}$	$S_{\max,\text{ref}}$	$\frac{p_{\max}}{p_{\max,\text{ref}}}$	$\frac{S}{S_{\max,\text{ref}}}$	$\frac{t_c}{t_{f,\text{ref}}}$	$\frac{T_j}{563\ \text{K}}$
1	3.45%	152.0	1.5	0.663284	1.0	0.0	0.952140
2[a]	3.45%[c]	152.0	1.5	0.714286	1.0	0.0	0.957383
3[a]	3.45%[c]	152.0	1.5	0.425188	0.715	0.056	0.879339
4[a]	3.45%[c]	152.0	1.5	0.412343	0.515	0.102	0.901480
5	2.52%	156.0	2.0	0.658932	1.0	0.0	0.960214
6	4.43%	150.0	1.5	0.702556	1.0	0.0	0.960214
9	3.45%	152.0	5.5	0.700000	1.0	0.0	0.980000

[a c]: V_T-constrained problem.

(a) solves a quadratic programming (QP) problem in which the nonlinear function, $\mathcal{F}$, is expanded around the feasible point by a quadratic function, and the nonlinear constraints are linearized, using Jacobians. The solution of this QP problem gives a search direction;

(b) obtains a step size in this direction which minimizes an augmented Lagrangian merit-function; and

(c) updates the approximate Hessian of the Lagrangian merit-function using a modified BFGS quasi-Newton method.

Initial estimates to the solution of the optimization problems, and the range of ε, must be supplied. These are given in Tables I and II. The values of the other important parameters required in the E04UCF code are given in Table III. All the partial derivatives required by the technique are generated numerically by the program. The CPU time taken for a typical run on a DEC ALPHA 3000/600 S mainframe computer is 1–5 min, depending upon the number of iterations, and the number of times the QP problem is solved in one iteration.

Table II Minimum Values for I_1 and I_2 [Eqs. (11) and (12)]

Problem No.	$[W]_0$	$\frac{t_f}{t_{f,\text{ref}}}$ [Eq. (11)]	$\frac{[C_2]_f}{[C_2]_{f,\text{ref}}}$ [Eq. (12)]
1	3.45%	0.4687150	0.1341986
2–4[a]	3.45%[a]	0.4687293	0.1346451
5	2.52%	0.4334147	0.1291566
6	4.43%	0.4933124	0.1426872
9	3.45%	0.4213532	0.1336732

[a] V_T-constrained problem.

RESULTS AND DISCUSSION

The reference values ($t_{f,\text{ref}}$, conv_f, and $[C_2]_{f,\text{ref}}$) were first generated using the simulation code developed by Wajge et al.[24] The feed conditions as well as some of the operating conditions used for manufacturing one grade of nylon 6 currently (being referred to as Problem 1) are[24]

Problem 1

$$[C_1]_{0,\text{ref}} = 8.54425\ \text{mol/kg}$$

$$[W]_{0,\text{ref}} = 1.91667\ \text{mol/kg}$$

(3.45%, by weight)

$$T_{0,\text{ref}} = 90°\text{C}$$

$$T_{j,\text{ref}} = 270°\text{C}$$

$$p_{0,\text{ref}} = 101.3\ \text{kPa} \quad (1\ \text{atm})$$

$$S_{\max,\text{ref}} = 1.5 \qquad (13)$$

Under these conditions, the value of $\mu_{n,\text{ref}}$ is 152.0. Other details are available in Ref. 24.

Figure 3 shows the Pareto set obtained for the $[W]_0 = 3.45\%$ case [Problem 1, eq. (13)] using the solutions of eqs. (11) and (12) as given in Table II. Increments of 0.01 for ε have been used in eq. (10b). It may be mentioned that the starting (guess) so-

Table III Parameters Used in the SQP Code

Parameters	Values
tol_{ob}	10^{-4}
tol_{ni}	10^{-4}
func_{pr}	10^{-10}
tol_{act}	10^{-8}

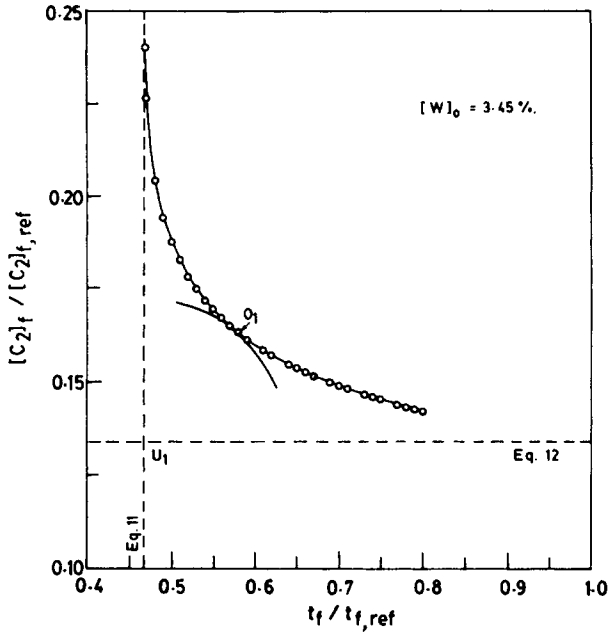

Figure 3 Pareto set for $[W]_0 = 3.45\%$, $\mu_{n,ref} = 152$. Circles show "exact" Pareto points while curve shows the smoothened, suboptimal Pareto. Utopia (U_1) and preferred solution (O_1) shown, along with solutions of problems in eqs. (11) and (12).

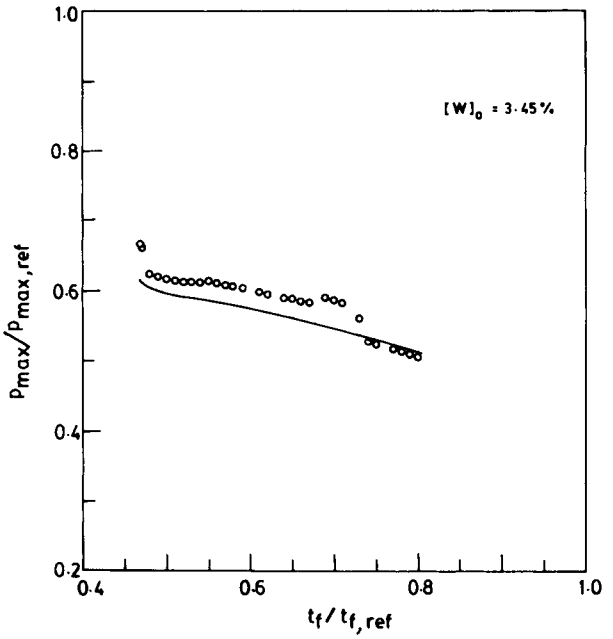

Figure 4 Optimal values of the dimensionless maximum pressure for the different cases shown in Figure 3. $[W]_0 = 3.45\%$.

lution for the first Pareto point corresponding to $\varepsilon = 0.47$ [eq. (10)] is that given in Table I. For subsequent values of ε (0.48, 49, . . .) studied, the guess solution is the optimal solution (on the Pareto set) for the previous value of ε. This "educated" starting guess for all points on the Pareto set (except the first) helps reduce the computer time considerably, without affecting the final results much.

Figure 3 shows that as the value of one objective function, $t_f/t_{f,ref}$, decreases (improves) the other one increases (worsens). The curve in Figure 3, thus, depicts the typical characteristics of a Pareto set. The corresponding optimal values of the control parameters, p_{max}, S, t_c, and T_j (in dimensionless form), corresponding to the different points of the Pareto in Figure 3, are shown in Figures 4–7 (circles). Some amount of scatter is observed in Figures 4–6, but the optimal values of T_j show a smooth decrease as $t_f/t_{f,ref}$ increases. In fact, some adjacent values of the optimal control parameters fluctuate wildly, even though the Pareto itself is quite smooth. This creates problems in the use of our optimization results in industry and needs further study. We found that changes in values of p_{max}, S, and t_c around their optimal values lead to relatively small changes in the values of $t_f/t_{f,ref}$ and $[C_2]_f/[C_2]_{f,ref}$. This suggests that we can obtain *smoothened* curves for the operating (control) parameters (instead of the fluctuating points shown by circles in Figs. 4–6) and still be quite close to Pareto solutions. These *suboptimal* solutions would have more use in industrial practice.

The suboptimal Pareto set was generated by fixing S and $t_c/t_{f,ref}$ at 1.5 and 0.025, respectively, and obtaining values of $p_{max}/p_{max,ref}$ and T_j by solving the following problem:

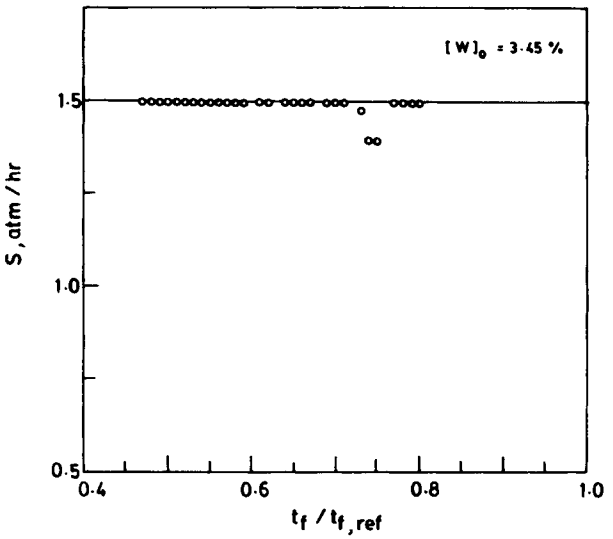

Figure 5 Optimal |slope| for the different cases shown in Figure 3. $[W]_0 = 3.45\%$.

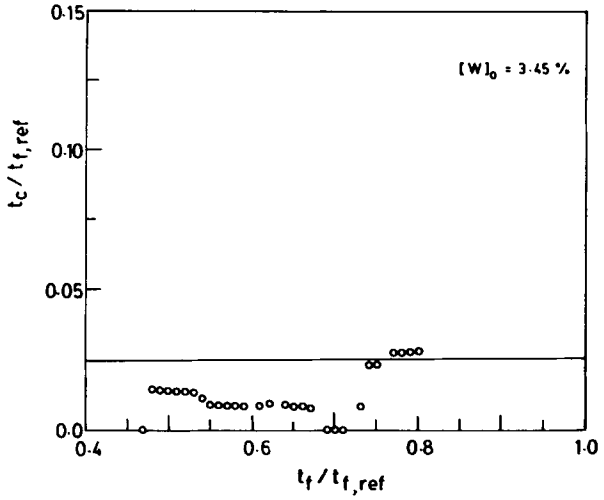

Figure 6 Optimal $t_c/t_{f,ref}$ for the different cases shown in Figure 3. $[W]_0 = 3.45\%$.

$$\text{Min } I(p_{max}/p_{max,ref}, T_j) = \left[\frac{[C_2]_f}{[C_2]_{f,ref}} - \left(\frac{[C_2]_f^P}{[C_2]_{f,ref}^P}\right)_i\right]^2; \quad i = 1, 2, 3, \ldots, N^P \quad (14a)$$

s.t.:

$$t_f/t_{f,ref} = (t_f^P/t_{f,ref}^P)_i \quad (14b)$$

constraint eqs. (9b)–(9e) and (9h) (14c)

In this equation, the superscript, P, indicates the points on the original Pareto set comprising N^P points. The problem described in eq. (14a) generates (sub)optimal values of $p_{max}/p_{max,ref}$ and T_j which give points on Figure 3 which do not deviate much from the original Pareto. The suboptimal solutions are shown by smooth curves in Figures 3–7. It is observed from Figure 3 that the suboptimal (smoothened) Pareto is almost indistinguishable from the original Pareto, even though some of the parameter values differ from their original values considerably. It may be added that the constant (smoothened) values of S and $t_c/t_{f,ref}$ have been selected after some trial and error, to ensure convergence of results as well as to obtain reasonably low deviations from the original Pareto.

An interesting variation of the problem described in eq. (9) was to see if addition of one *more* constraint on the *maximum* rate of release of vapors, $V_{T,max}$, leads to any changes in the results. If the control valve in the industrial reactor is working at its maximum capacity, $V_{T,max,ref}$ (mol/h), then $V_{T,max}/V_{T,max,ref}$ would be limited to lie below unity. Thus, the following *additional* constraint could be incorporated in Eqs. (9)–(12):

Problem 2

$$V_{T,max}/V_{T,max,ref} \leq 1 \quad (15)$$

The results of this problem, referred to as the V_T-constrained problem, generated using the information given in Tables I–III, are shown in Figures 8–12. A larger amount of scatter is observed in the curves showing the optimal values of the parameters than in Problem 1. However, the suboptimal Pareto obtained using $S = 1.5$ and $t_c/t_{f,ref} = 0.015625$, and solving the problem described in eq. (14) [with the constraint of eq. (15) included], is again observed (curve in Fig. 8) to lie close to the original Pareto set. It is interesting to observe that the suboptimal Pareto in Figure 8 is almost identical to that in Figure 3, even though values of $V_{T,max}/V_{T,max,ref}$ go beyond 1.0 for the points on the original Pareto. The optimal value of T_j also is observed to be almost identical for the V_T-constrained and unconstrained problems.

We now decided to study the sensitivity of the Pareto set to the initial guess used. The V_T-constrained problem was solved again, this time starting from the high $t_f/t_{f,ref}$ end (Problem 3). The guess solution used is given in Table I (Problem 3).

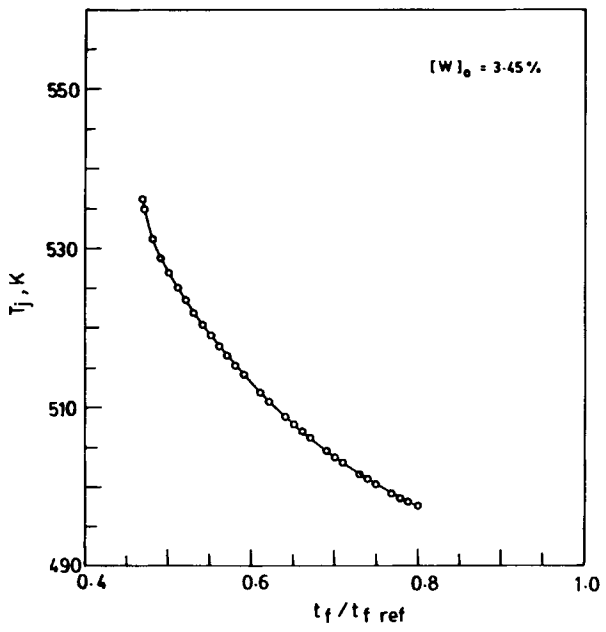

Figure 7 Optimal jacket temperature for the different cases shown in Figure 3. $[W]_0 = 3.45\%$.

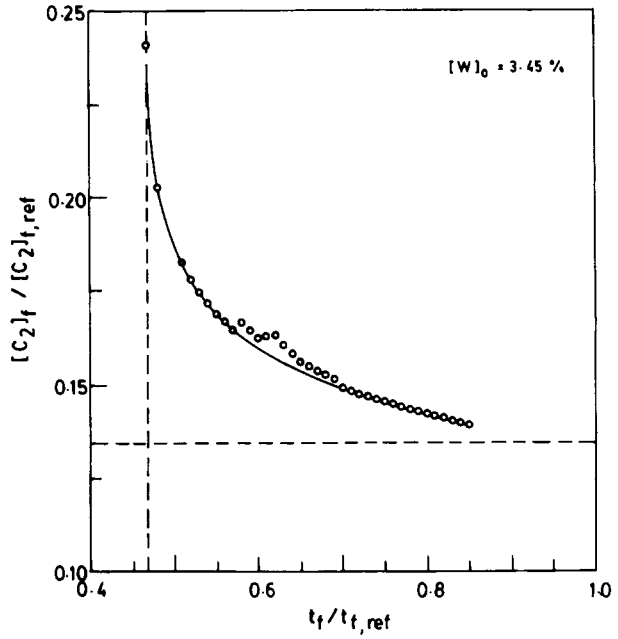

Figure 8 Pareto set with V_T-constraint included, for $[W]_0 = 3.45\%$, $\mu_{n,ref} = 152$. Other notations as in Figure 3.

The corresponding Pareto set (reverse) is shown in Figure 13 by triangles. Another set of Pareto points (Problem 4) was generated, starting close to the midpoint of the Pareto in Figure 3. The initial guesses for this problem are given in Table I, and

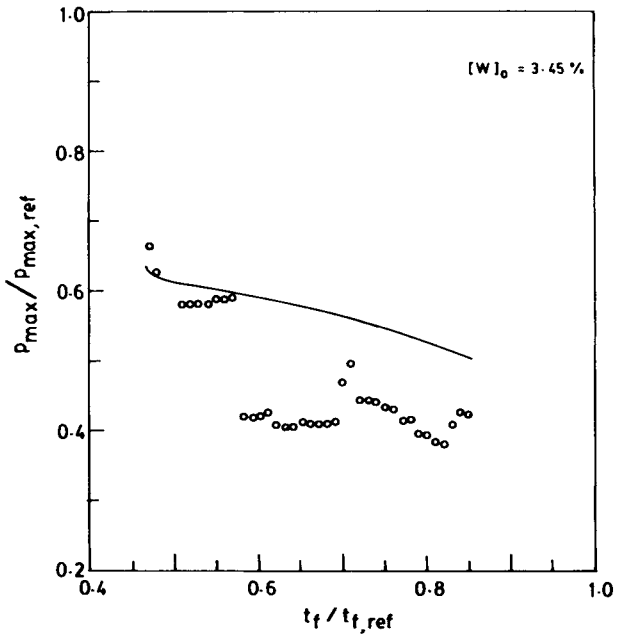

Figure 9 Optimal values of the dimensionless maximum pressure for the different cases shown in Figure 8. $[W]_0 = 3.45\%$.

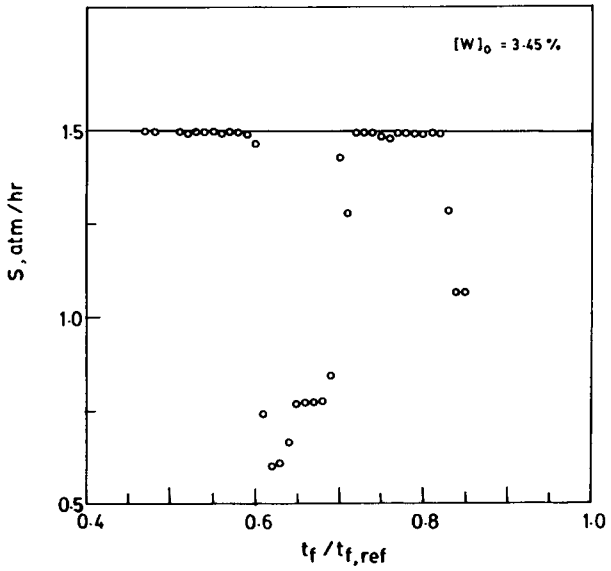

Figure 10 Optimal |slope| for the different cases shown in Figure 8. $[W]_0 = 3.45\%$.

the Pareto set (midpoint) is shown by crosses in Figure 13. The initial guess is observed to affect the Pareto somewhat. Indeed, the SQP method used for generating the optimal solutions has first-order convergence characteristics, and it is not possible to obtain *exact* results numerically, since the rate of convergence becomes extremely sluggish as one approaches the solution. This is why slightly different

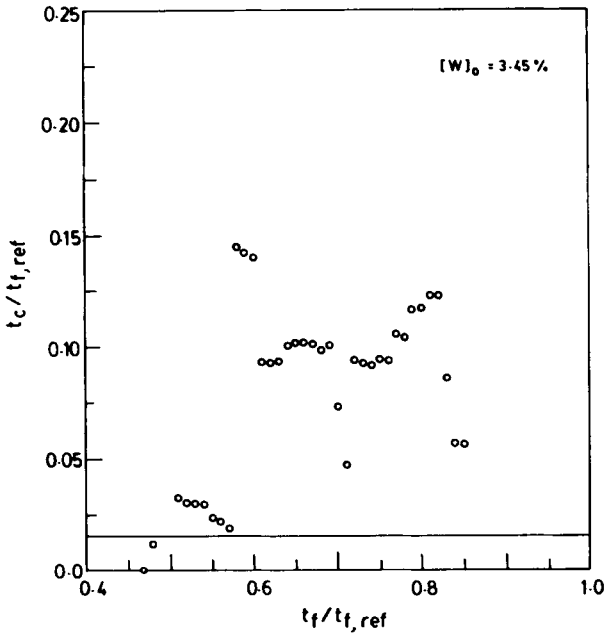

Figure 11 Optimal $t_c/t_{f,ref}$ for the different cases shown in Figure 8. $[W]_0 = 3.45\%$.

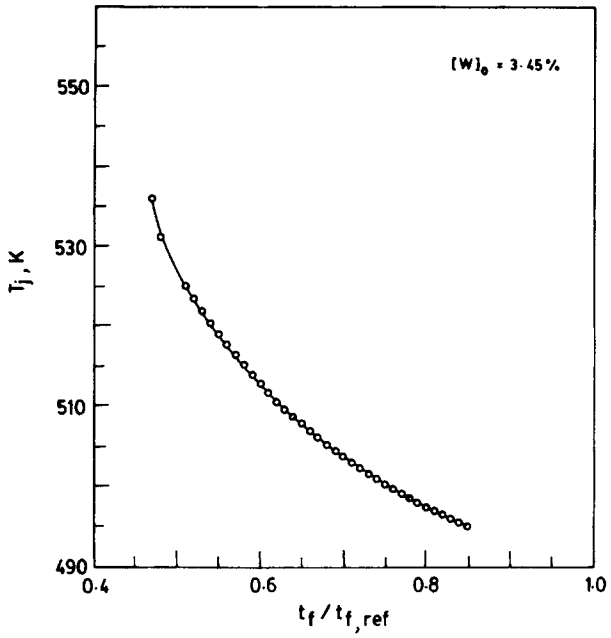

Figure 12 Optimal jacket temperature for the different cases shown in Figure 8. $[W]_0 = 3.45\%$.

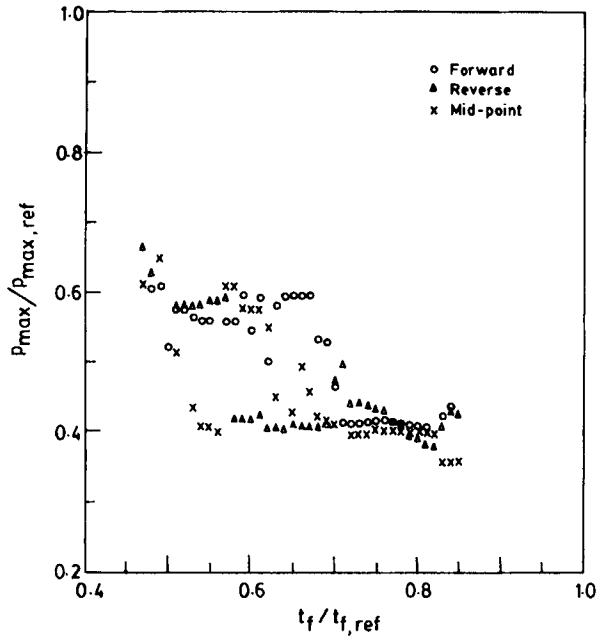

Figure 14 Optimal values of the dimensionless p_{max} for the three Paretos of Figure 13.

numerical results are obtained for the Pareto set, depending on the initial guess used. Strictly speaking, therefore, when first-order computer methods are used to generate the solutions to the optimization problem, one can at best obtain a suboptimal, narrow *Pareto band.* The (sub)optimal values of the parameters, also, depend on the choice of the initial conditions. Figures 14–16 show results on the optimal values of the operating parameters, obtained for the different Pareto sets in Figure 13. Optimal

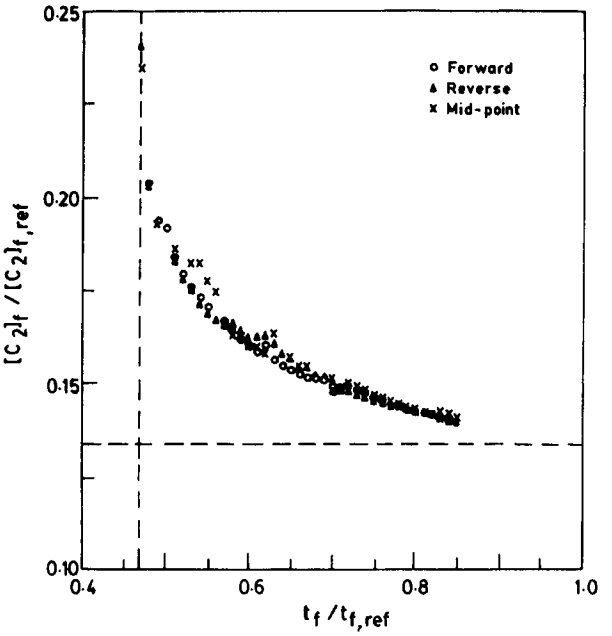

Figure 13 "Exact" Paretos for the V_T-constrained problem, as obtained from different starting guesses. $[W]_0 = 3.45\%$, $\mu_{n,ref} = 152$.

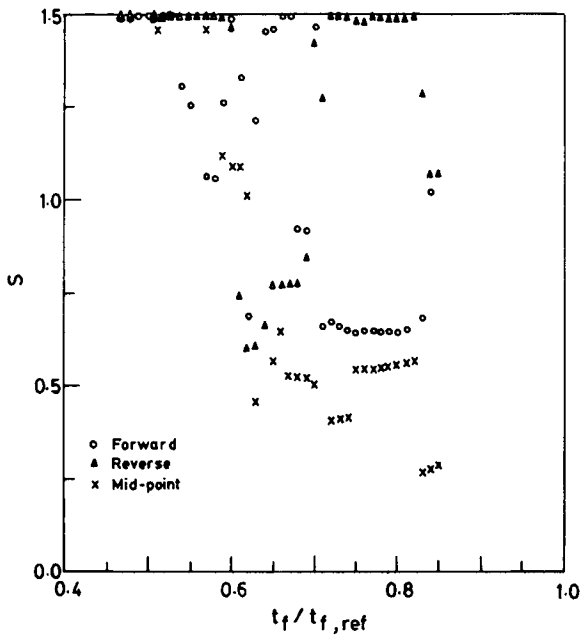

Figure 15 Optimal values of the |slope| for the three Paretos of Figure 13. Some crosses on the upper border have not been shown for clarity.

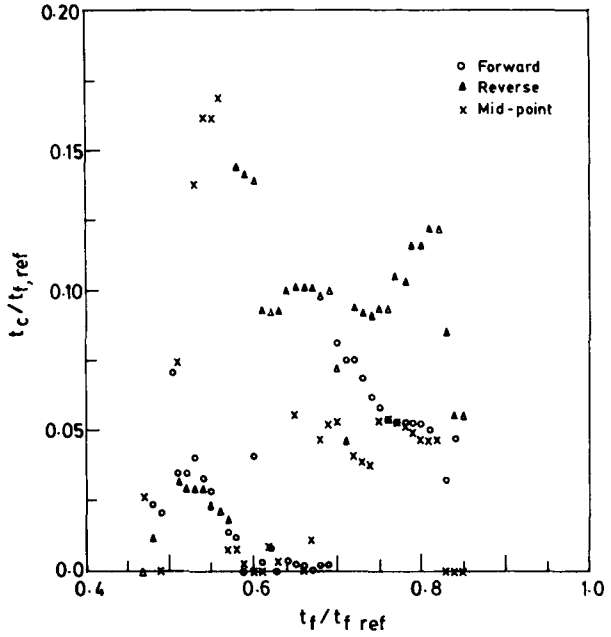

Figure 16 Optimal values of $t_c/t_{f,ref}$ for the three Paretos of Figure 13.

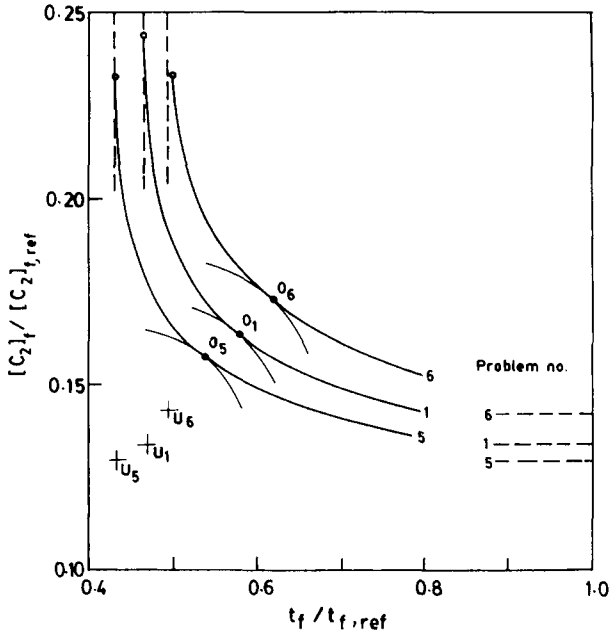

Figure 17 Unconstrained, smoothened Paretos for the three grades of nylon 6 produced presently. Problem numbers described in Table I. Utopia and preferred solutions shown along with limiting values obtained using eqs. (11) and (12). Values of $[W]_0$, $\mu_{n,f}$, and $\text{conv}_{f,ref}$ differ for the three cases.

values of T_j are almost unaffected by the choice of the starting point, and Figure 12 holds for all cases. In view of the scatter observed in Figures 13–16, generating suboptimal Paretos using the smoothening technique [eq. (14)] appears justified.

Suboptimal (smoothened) Pareto solutions (without V_T-constraints) were generated for the two other grades[24] of polymer being produced currently in the industrial reactor. These correspond to a different set of values of $[W]_0$, conv_f, $\mu_{n,ref}$, and $S_{max,ref}$, some of which are given in Table I (Problems 5 and 6). The initial guesses and the solutions of the associated limiting optimal problems [eqs. (11) and (12)] are given for these cases in Tables I and II. Values of $p_{o,ref}$ and $T_{o,ref}$ are the same as in eq. (13). The Pareto sets are given in Figure 17 (only the smoothened Pareto sets are shown). The values of $[C_2]_{f,ref}$ used for nondimensionalization are slightly different for the three cases shown and correspond to currently produced concentrations of the cyclic dimer in the different batches. The trends, however, remain the same, even if we plot $[C_2]_f$ rather than the dimensionless values. Figure 18 shows the optimal (smoothened) values of the operating parameters for these cases. Smoothened values of S and $t_c/t_{f,ref}$ for these problems are given in Table IV. It is to be noted that one can achieve *substantial* improvements in the operation of the industrial reactor in all three cases studied herein, merely by effecting simple changes in the operating variables in the industrial reactor.

The Pareto sets in Figure 17 correspond to different values of $[W]_0$, $\mu_{n,ref}$, and conv_f, as practiced in the industrial situation currently [by varying $p(t)$,

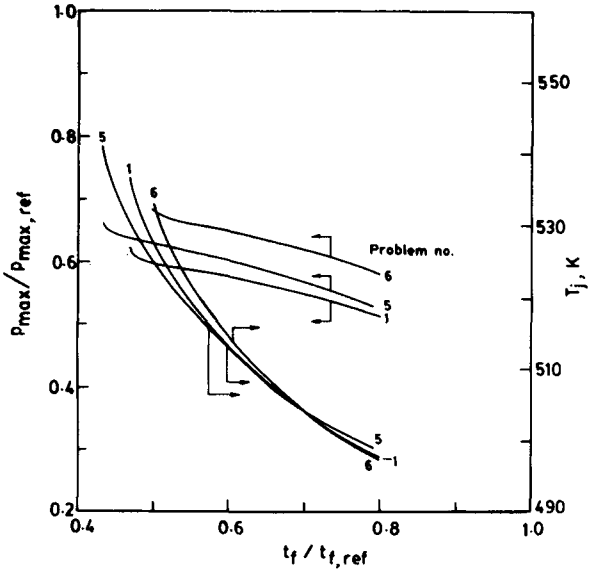

Figure 18 Optimal (smoothened) values of $p_{max}/p_{max,ref}$ and jacket fluid temperature for the Paretos of Figure 17.

Table IV Smoothened Optimal Values of S and $t_c/t_{f,ref}$

Problem No.	S (atm/h)	$t_c/t_{f,ref}$
1	1.5	0.025
2[c]	1.5	0.015625
5	2.0	0.0000625
6	1.5	0.00625

but using the same t_f]. An interesting result is obtained when we generate Pareto sets (in the absence of V_T-constraints), keeping $\mu_{n,f}$ fixed at 152.0 and the monomer conversion constant at the reference value of Problem 1 and varying $[W]_0$ *alone*. A study of Pareto sets so generated (Fig. 19, near the central region) reveals that the value of $[W]_0 = 3.45\%$ presently being used to manufacture this grade ($\mu_{n,f} = 152$) of polymer appears to be the best and that increasing $[W]_0$ substantially would lead to a worsening of the operation.

As indicated earlier, with the generation of the Pareto sets, the mathematical phase of the problem is over. A decision maker (DM) can now select a "preferred" solution from among the equivalent optimal points on the Pareto. A simple and widely used technique for doing this is the Surrogate Worth Trade-Off Method. The slope of the Pareto, $\partial I_i/\partial I_j$, at any point represents a trade-off value between the objectives I_i and I_j quantitatively. The DM assigns weights (in the range -10 to $+10$) to each point on the Pareto, looking at the slopes as well as using his or her judgment (usually nonquantifiable). The magnitude of the assigned weight depends on how strongly the DM favors or rejects the trade-off. The preferred solution finally selected is the one to which the DM (or DMs, each assigning weights independently, before an averaging is done) has assigned a weight of zero, i.e., the DM feels that at the preferred point the gains and losses of moving away balance each other. The Pareto helps narrow down the focus of the DM to a selected number of equivalent optimum points and channelizes the thought processes of the DM in a better manner.

A simpler and more mathematical approach is to select the preferred solution as a point nearest to a point called utopia. This is the point whose coordinates are the solutions of Eqs. (11) and (12). This point is, obviously, unattainable, but represents an ideal. Choosing a (feasible) point on the Pareto nearest this point is a reasonable choice, in the absence of additional information usually constituting one's "judgment." Figure 3 shows the utopia (U_1) as well as the preferred solution (O_1). Figure 17 shows these points for the three grades of polymer being produced. Table V gives more detailed information on the three preferred solutions shown in Figure 17. Also included in this table (as Problems 7 and 8) are optimal solutions for Problems 1 and 2 as obtained by us earlier[30] for the $[W]_0 = 3.45\%$ case, using only three control variables, $p_{max}/p_{max,ref}$, S, and $t_c/t_{f,ref}$ (and not T_j, which was fixed at 270°C). A one-variable search optimization technique was used in our previous study with "judgment" used to ascertain the best point (rather than use multiobjective function optimization). It is observed that our earlier study led to a slightly better optimum point (both $[C_2]_f/[C_2]_{f,ref}$ and $t_f/t_{f,ref}$ are better; see Table V, Problems 1 and 7), but it must be mentioned that the value of S_{max} was much higher compared to that used in the present study, in which S_{max} is kept at the current operating value of $S_{ref} = 1.5$. Higher values of S in Problem 7 lead to higher maximum values of the vapor release rate. Use of a higher permissible range of S, $0 \le S \le 5.5$, with the current technique (multiobjective function optimization) leads to the preferred solution given in Table V (Problem 9). The values of both $[C_2]_f$ and t_f are found to be worse than in Problem 7.[30] However, the value of $conv_f/conv_{f,ref}$ in Problem 7 is lower at 0.9897 than in Problem 9, for which it is 1.0 ± 0.0001.

Figure 20 shows how μ_n varies with $t/t_{f,ref}$ for the operating conditions used currently,[24] as well as for

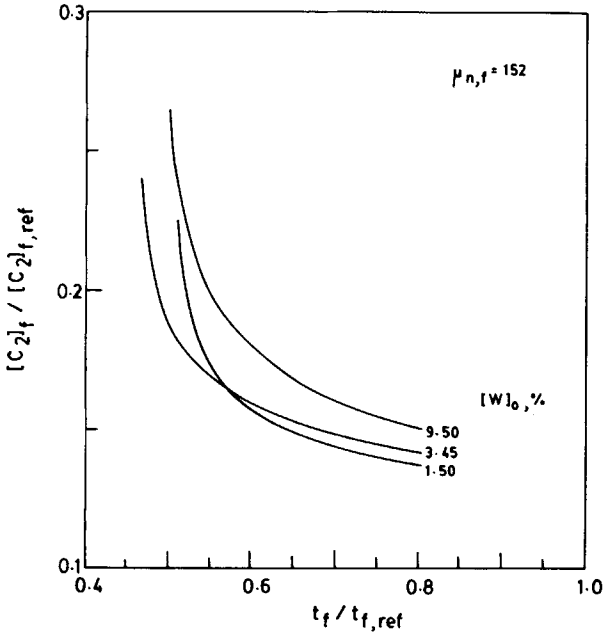

Figure 19 Smoothened Paretos for the case of $\mu_{n,f} = 152$, with $[W]_0$ varied but $conv_{f,ref}$ remaining the same for all cases.

Table V Preferred Solutions from the Pareto Sets

Problem No.	$[W]_0$	$\mu_{n,ref}$	$\frac{[C_2]_f}{[C_2]_{f,ref}}$	$\frac{t_f}{t_{f,ref}}$	$\frac{p_{max}}{p_{max,ref}}$	S	$\frac{t_c}{t_{f,ref}}$	T_j (°C)	$\frac{V_{T,max}}{V_{T,max,ref}}$
5	2.52%	156.0	0.156	0.55	0.599	1.81	0.003295	244.91	1.547
1	3.45%	152.0	0.163	0.58	0.606	1.50	0.008984	242.26	0.858
6	4.43%	150.0	0.172	0.62	0.647	1.455	0.0006378	239.13	0.851
7	3.45%[30]	152.0	0.156	0.405	0.829	5.5	0.0	270.00[a]	1.700
8[b]	3.45%[30]	152.0	0.181	0.407	0.60	2.5	0.05	270.00[a]	0.985
9	3.45%	152.0	0.165	0.55	0.766	5.5	0.0	246.23	1.770

[a] Assumed.
[b] V_T-constrained case.

the preferred solutions (Problem 1, 5, and 6 in Table V). It is interesting to note that optimal operation leads to a vanishing of the intermediate plateau in the $\mu_n(t)$ plots. Also, μ_n does not attain its final value, $\mu_{n,ref}$, asymptotically for the optimal cases, and, so, better control of the emptying operation of the reactor is required to prevent the overshoot of μ_n. Such control should not pose much problem these days. Figure 21 shows the variation of the temperature of the reaction mass for the current operation, as well as for the optimal cases (preferred solutions in Table V). The temperature history, $T(t)$, for the optimal solution differs from what is currently practiced, because of differences in the rates of vaporization necessitated by different pressure histories. These trends are similar, *qualitatively*, to what was predicted for the optimal conditions in our previous work.[30]

CONCLUSIONS

In this article, multiobjective Pareto optimal solutions have been generated for an industrial nylon 6 reactor for producing three different grades of polymer. Operating variables have been generated corresponding to the preferred optimal solutions for all three cases. These can be implemented on the in-

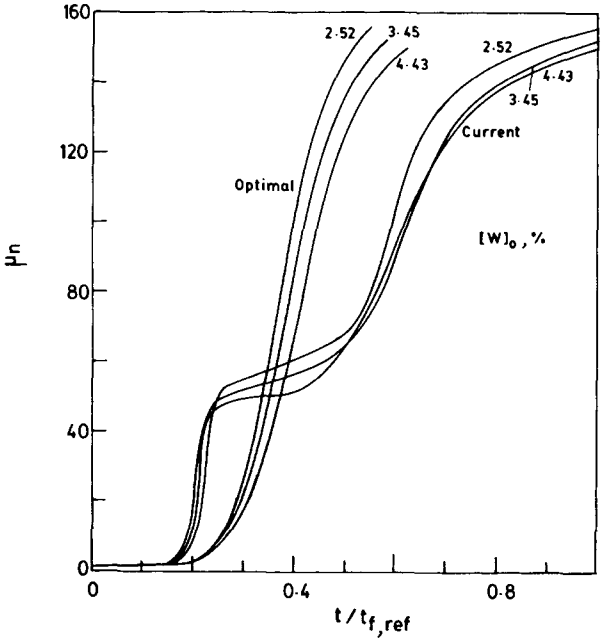

Figure 20 Variation of the degree of polymerization with dimensionless time for the current and optimal (preferred solution) cases, for the three grades of nylon 6 produced (see Fig. 17).

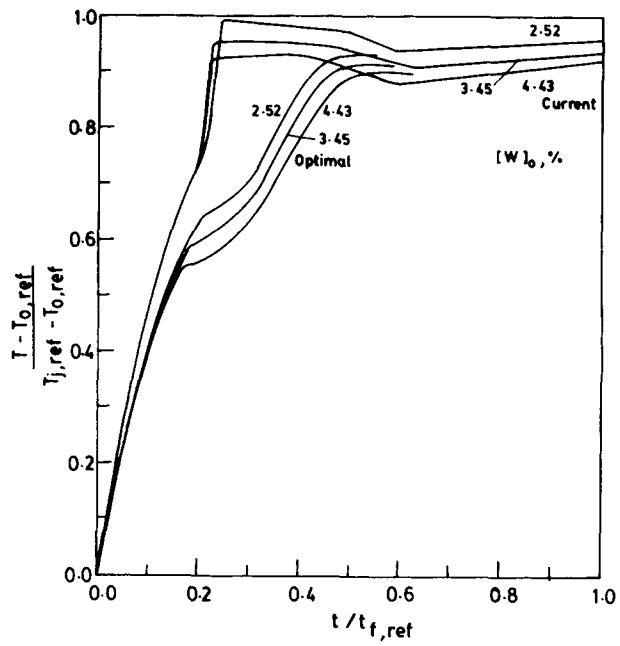

Figure 21 Variation of the dimensionless temperature with dimensionless time for the current and optimal (preferred solution) case, for three grades of nylon 6, as in Figure 17.

dustrial unit quite easily and lead to substantial improvements over the present situation. The methodology used is better than that used in our previous study, where individual judgment was used to decide upon the best point. The technique can easily be applied or extended to other industrial polymerization reactors, even though our focus has been on a particular kind of a nylon 6 semibatch reactor.

This work has been partly funded by a grant from the Research Center, Gujarat State Fertilizers Co. Ltd., Vadodara, India.

NOMENCLATURE

$[C_i]$	concentration of caprolactam ($i = 1$) and cyclic dimer ($i = 2$) in liquid phase (mol/kg mixture)
$[C_2]^P_{f,i}$	nondimensionalized final dimer concentration, $[C_2]_f/[C_2]_{f,\text{ref}}$, corresponding to ith point on Pareto
conv	monomer conversion [eq. (7)]
DP	degree of polymerization of polymer product
F	mass of liquid in reactor at time t (kg)
$\mathcal{F}$	general, nonlinear function
func_{pr}	precision for function evaluation
I	vector of objective functions, I_i
n	no. equations
N^P	no. points on Pareto
PDI	polydispersity index
p	pressure (kPa or atm)
S	slope (absolute value) of pressure vs. time plot during the third stage in reactor being optimized (atm/h)
t	time (h)
t_c	time for which pressure remains constant at $p_{\max}$ (h)
t_f	total reaction time (h)
$t^P_{f,i}$	nondimensionalized reaction time, $t_f/t_{f,\text{ref}}$, corresponding to ith point on Pareto
T	temperature (K)
TOL	tolerance in D02EJF code of NAG library
u	vector of control variables, u_i
V_T	rate of vapor release from reactor (mol/h)
$[W]$	water concentration in liquid (mol/kg mixture)
x	vector of state variables, x_i

Greek Letters

μ_i	ith moment of the chain length distribution ($i = 0, 1, 2, \ldots$)
μ_n	number-average chain length ($\equiv \mu_1/\mu_0$)
$\prod$	dimensionless pressure [eq. (6)]
τ	dimensionless time [eq. (6)]
ζ_1	total moles of monomer vaporized in reactor until time t (mol)

Subscripts/Superscripts

act	active constraints
c	V_T-constrained problem
f	final (value for the product)
j	jacket
L	linear constraints
max	maximum value
nl	nonlinear constraints
0	feed conditions
ob	objective function
pr	precision
p	Pareto
ref	reference (value used in industrial reactor currently)

REFERENCES

1. J. N. Farber, in *Handbook of Polymer Science and Technology*, N. P. Cheremisinoff, Ed., Marcel Dekker, New York, 1989, Vol. 1, p. 429.
2. B. M. Louie and D. S. Soong, *J. Appl. Polym. Sci.*, **30,** 3707 (1985).
3. M. E. Sachs, S. I. Lee, and J. A. Beisenberger, *Chem. Eng. Sci.*, **27,** 2281 (1972).
4. J. N. Farber and R. L. Laurence, *Chem. Eng. Commun.*, **46,** 347 (1986).
5. J. Hicks, A. Mohan, and W. H. Ray, *Can. J. Chem. Eng.*, **47,** 590 (1969).
6. P. J. Hoftyzer, J. Hoogschagen, and D. W. van Krevelen, in *Proceedings of the 3rd European Symposium on Chemical Reaction Engineering*, Amsterdam, Sept. 15–17, 1964, p. 247.
7. H. K. Reimschuessel and K. Nagasubramanian, *Chem. Eng. Sci.*, **27,** 1119 (1972).
8. W. F. H. Naudin ten Cate, in *Proceedings of the International Congress in Use of Elec. Comp. in Chem. Eng.*, Paris, April 1973.
9. S. Mochizuki and N. Ito, *Chem. Eng. Sci.*, **33,** 1401 (1978).
10. A. Ramagopal, A. Kumar, and S. K. Gupta, *J. Appl. Polym. Sci.*, **28,** 2261 (1983).
11. S. K. Gupta, B. S. Damania, and A. Kumar, *J. Appl. Polym. Sci.*, **29,** 2177 (1984).

12. A. K. Ray and S. K. Gupta, *J. Appl. Polym. Sci.*, **30,** 4529 (1985).
13. A. K. Ray and S. K. Gupta, *Polym. Eng. Sci.*, **26,** 1033 (1986).
14. D. Srivastava and S. K. Gupta, *Polym. Eng. Sci.*, **31,** 596 (1991).
15. Y. Y. Haimes, *Heirarchial Analysis of Water Resources Systems,* McGraw-Hill, New York, 1977.
16. V. Chankong and Y. Y. Haimes, *Multiobjective Decision Making—Theory and Methodology,* Elsevier, New York, 1983.
17. A. Tsoukas, M. Tirrel, and G. Stephanopoulos, *Chem. Eng. Sci.*, **37,** 1785 (1982).
18. L. T. Fan, C. S. Landis, and S. A. Patel, in *Frontiers in Chemical Reaction Engineering,* L. K. Doraiswamy and R. A. Mashelkar, Eds., Wiley Eastern, New Delhi, 1984, p. 609.
19. J. N. Farber, *Polym. Eng. Sci.*, **26,** 499 (1986).
20. D. Butala, K. Y. Choi, and M. K. H. Fan, *Comput. Chem. Eng.*, **12,** 1115 (1988).
21. R. M. Wajge and S. K. Gupta, *Polym. Eng. Sci.*, **34,** 1161 (1994).
22. A. Gupta, S. K. Gupta, K. S. Gandhi, B. V. Ankleswaria, M. H. Mehta, M. R. Padh, and A. V. Soni, in *Recent Trends in Chemical Reaction Engineering,* B. D. Kulkarni, R. A. Mashelkar, and M. M. Sharma, Eds., Wiley Eastern, New Delhi, 1987, p. 281.
23. A. Gupta, S. K. Gupta, K. S. Gandhi, M. H. Mehta, M. R. Padh, A. V. Soni, and B. V. Ankleswaria, *Chem. Eng. Commun.*, **113,** 63 (1992).
24. R. M. Wajge, S. S. Rao, and S. K. Gupta, *Polymer,* **35,** 3722 (1994).
25. S. K. Gupta, in *Handbook of Polymer Science and Technology,* N. P. Cheremisinoff, Ed., Marcel Dekker, New York, 1989, Vol. 1, p. 211.
26. S. K. Gupta, *Numerical Methods for Engineers,* Wiley Eastern/New Age International, New Delhi, 1995.
27. W. H. Ray and J. Szekely, *Process Optimization,* Wiley, New York, 1973.
28. P. E. Gill, W. Murray, and M. H. Wright, *Practical Optimization,* Academic Press, New York, 1981.
29. P. E. Gill, S. J. Hammerling, W. Murray, M. A. Saunders, and M. H. Wright, *User's Guide for LSSOL,* Stanford University, Report SOL 86-1, 1986.
30. R. Sareen, M. R. Kulkarni, and S. K. Gupta, *J. Appl. Polym. Sci.*, **57,** 209 (1995).

Received May 10, 1995
Accepted June 4, 1995